

Lightning arc channel effects on surface damage development on a PRSEUS composite panel: An experimental study

Dounia Boushab,^a Pedram Gharghabi,^b Juhyeong Lee,^c Thomas E. Lacy Jr.,^{a*} Charles U. Pittman Jr.,^d Michael S. Mazzola,^e Alexander Velicki^f

^aTexas A&M University, J. Mike Walker '66 Department of Mechanical Engineering, College Station, TX, 77843

^bTesla, Palo Alto, CA, 94304

^cUtah State University, Department of Mechanical & Aerospace Engineering, Logan, UT, 84322

^dMississippi State University, Department of Chemistry, Starkville, MS, 39762

^eUniversity of North Carolina, Department of Electrical and Computer Engineering, Chapel Hill, NC, 28223

^fThe Boeing Company (Retired), Huntington Beach, CA, 92647

Abstract. Composite aircraft structures are vulnerable to lightning strike damage due to their relatively low electrical and thermal conductivities. A preceding work has investigated the lightning damage resistance of a carbon-epoxy Pultruded Rod Stitched Efficient Unitized Structure (PRSEUS) panel. The damage includes intense local damage (*i.e.*, matrix decomposition/sublimation, fiber rupture, delamination) accompanied by widespread surface damage (*i.e.*, distributed fiber rupture and tow splitting) further from the lightning attachment point. This study focuses on investigating the cause of the widespread surface damage. Two possible driving mechanisms are explored: *i*) magnetically-induced currents and *ii*) lightning arc-root/channel expansion. Fifteen laboratory-scale lightning strike tests at nominal peak currents of 50-125 kA were performed on modified PRSEUS mid-bay locations. The surface modifications were placed adjacent to or enclosing the intended lightning arc attachment point, including through-slots, a non-conductive silicon-filled slot, insulating tape, and acrylic plates. The objective is to examine the effect of such barriers on lightning-induced surface damage for cases where the anisotropic lightning arc-root/channel expansion and/or the lightning arc primary current are constrained by the barriers, without affecting the magnetically-induced currents. In each of the lightning strike tests, both the intense local damage and widespread surface damage were limited by or enclosed within the insulating boundary. The placement of these boundaries altered the lightning arc-channel expansion or limited the interaction between the expanding-arc and the surface of the PRSEUS panel. These experiments demonstrate that the widespread surface damage outside of the attachment point primarily results from lightning arc-root/channel expansion rather than magnetically induced currents.

Keywords: PRSEUS, lightning damage, arc attachment, stitched carbon-epoxy composite, lightning arc-channel expansion, magnetically-induced currents.

*Corresponding author.

E-mail address: telacyjr@tamu.edu

1 Introduction

In-flight lightning strike damage to aircraft primary structures is a serious concern, which may compromise aircraft airworthiness. During a lightning strike, a significant amount of electrical energy and kinetic energy is instantaneously absorbed/dissipated in a localized area surrounding the lightning attachment point, resulting in significant thermal and mechanical damage due to a combination of resistive (Joule) heating, electromagnetic “Lorentz” force, and shockwaves. Lightning can also induce detrimental “indirect” effects, including interference with electronic systems due to the induced electromagnetic field, internal arc discharge (caused by large potential differences), sparking, and ignition of vapor in fuel tanks [1].

The temperature of a typical lightning arc-channel can approach 30,000°K [2]. Thus, the air surrounding the lightning channel is rapidly heated, which results in a shock wave that propagates radially outward from the center of the arc. While traditional aerospace-grade metallic structures are highly conductive, carbon fiber-reinforced polymer (CFRP) composites have much lower electrical conductivities due to the dielectric (insulating) behavior of the polymer matrix embedding the fibers. For instance, carbon-epoxy composites have a higher electrical resistivity ($2.5\text{--}15 \times 10^{-5} \Omega\text{m}$ [3-5]) than a typical aluminum alloy ($5.2 \times 10^{-8} \Omega\text{m}$ [3]), which exacerbates intense Joule (resistive) heating due to lightning strike. Once the local composite temperature at the attachment point exceeds the epoxy matrix decomposition temperature (300–500°C) [6, 7], the matrix decomposes/pyrolyzes, leading to char formation, and markedly degrades matrix/fiber interfaces. Also, inter-ply matrix vaporization can result in an explosive release of pressurized gases [8, 9]. Typically, various cured thermoset matrices start degrading at much lower temperatures (182–600°C) than the carbon fiber sublimation temperature (3316°C) [10]. Large temperature gradients may exist between the center of the relatively conductive carbon fiber tows and the dielectric matrix. For instance, as the degree of Joule heating increases, individual carbon fiber filaments may sublime (*i.e.*, directly transitioning from a solid phase into a gas) once their surface temperature exceeds 3000°C [10, 11]; void/cavity formation at the sublimation site can lead to tow splitting. Also, significant increases in local composite temperatures coupled with the coefficient of thermal expansion (CTE) mismatches between matrix and fiber (carbon has a negative CTE) can lead to large-scale fiber rupture and tow splitting. In addition, a significant transient mechanical shockwave overpressure occurs at the attachment point, resulting in localized fiber fractures, matrix cracking delamination, and other mechanical damage [12] that can couple with thermal damage. In general,

composite thermal damage due to lightning strike (matrix decomposition, fiber sublimation/ablation, fiber rupture, *etc.*) is more severe than corresponding mechanical damage due to lightning-induced magnetic forces and shockwave overpressure pulses emanating from the lightning arc-channel [3, 13-15].

Several researchers have studied and modeled the evolution of a lightning arc-channel, but only a few experimental investigations exist. For example, Wang *et al.* [16] performed three-dimensional (3D) magnetohydrodynamic (MHD) simulations to characterize the evolution of a 200 A lightning arc current in open air. The lightning arc temperature distribution was symmetric about the central channel axis, and the maximum temperature at the core of the channel was 23,000°K. Upon attachment to a simulated copper plate, the lightning arc plasma assumed a bell-shape with a peak radius of 50 mm that was influenced by the Lorentz force (*i.e.*, the force exerted by a magnetic field) and Joule heating. Larsson *et al.* [17] developed an arc-column model that predicted the thermodynamic behavior of a lightning arc-core. The arc-channel was assumed to be symmetric, and the plasma was modeled as a Newtonian fluid. The predicted temperature-time profile showed that the lightning arc-channel radius for a 100 A strike expanded quickly from 20 to 60 mm during the initial 80 ms. Also, Lago *et al.* [18] simulated the evolution of a lightning arc plasma to assess the degradation of a cross-ply carbon-epoxy composite laminate subjected to 200 and 800 A for a duration of 1 and 0.25 s, respectively. The simulated composite was 30 mm wide and 2 mm thick. The maximum temperatures of the 200 and 800 A lightning plasmas were 18,000 and 28,000°K, respectively. The predicted damage to the composite panel was more prominent at the surface than through the thickness (*i.e.*, for 200 and 800 A strikes, the in-plane surface damage radii were 5.8 and 7.7 mm, while the through-thickness damage depths were 0.3 and 0.4 mm, respectively). In addition, Herziger *et al.* [19] developed an analytical solution to describe the dynamic behavior of a radially expanding lightning arc channel in terms of the current intensity (50–1000 A) and duration (20–100 ns). Experimental lightning arc discharge initiated several “streamers” with diameters ranging from 0.5×10^{-3} to 1×10^{-3} cm, which combined to form a homogenous free arc. The number of individual streamers was strongly dependent on the dielectric strength of air and the applied voltage across the gap. The predicted shape of the expanding lightning arc was similar to a detonation in open air [19]. The homogeneous expansion of the lightning arc started at a radius of 5×10^{-3} cm. The lightning arc-expansion radial velocity decreased as the arc-column radius increased with time.

Martins [20] performed experiments to study the lightning arc-expansion of a 100 kA strike on the surface of both conductive and relatively non-conductive materials (*i.e.*, aluminum panels and Toray T700/M21 carbon-epoxy composite laminates). The arc shape, characteristic lengths, and the induced shock waves were analyzed. The influence of different surface coatings on the evolution of the arc-root (*i.e.*, the area in contact between the arc-channel and the material surface) at the attachment point were also evaluated. Figures 1a-b [20] show the *isotropic* expansion of the lightning arc-root upon encountering the surface of unpainted and painted aluminum panels, respectively. Once the lightning arc-root attached to the aluminum panel, the arc-root radial expansion velocity at the conductive aluminum surface was lower than that for the arc-column (*i.e.*, right above the root), resulting in a parabolic arc-root (Fig. 1a). When an insulating paint layer was added to the surface of the aluminum panel (Fig. 1b), the arc-root expanded for the first couple of microseconds following the arc-column expansion. As the surface paint started to decompose (after 12 μ s), the arc-root became concentrated and confined to an area with no paint. This, in turn, restricted the expansion of the arc-root (Fig. 1b). The insulating paint had a significant impact on the arc-root behavior, resulting in a more intense lightning arc in that confined area. Unlike the isotropic arc-roots induced on the two aluminum panels (Figs. 1a-b), the lightning arc-root at the composite surface had a complex *anisotropic* semi-conical shape that was influenced by the fiber orientation in the outermost ply (Figs. 1c-d). The arc-root expansion perpendicular to the fibers (Fig. 1d) was three times greater than that in the fiber direction (Fig. 1c). A distribution of regions with spot-like fiber damage occurred over the surface of the laminate [20] that were attributed to the arc-expansion perpendicular to the fibers.

Also, Kawakami [21] used a high-speed imaging camera to examine the lightning arc-expansion behavior on the surface of two (140 mm x 140 mm) square 16-ply Toray T700/2510 unidirectional carbon-epoxy laminates subjected to 30 kA nominal peak currents. Two opposite edges of each laminate were grounded with copper strips. The laminates were placed inside the current generator such that the carbon fibers were oriented either perpendicular or parallel to the grounding strips. In each case, the arc expansion parallel to the fiber direction was limited to a relatively narrow domain near the attachment point, whereas the rate and extent of arc expansion perpendicular to the fibers were significantly more *pronounced*. These results are consistent with those reported in reference [20]. By correlating the projected lightning arc flow area with the area containing visible surface erosion, the surface damage distribution was consistent with the path of arc-root expansion.

In this paper, lightning strike damage on resin-infused carbon-epoxy Pultruded Rod Stitched Efficient Unitized Structure (PRSEUS) panel was investigated. The National Aeronautics and Space Administration (NASA) Langley Research Center (LaRC) donated three PRSEUS panels for lightning strike testing. Each panel consisted of an outer skin reinforced with an underlying arrangement of periodically spaced stringers, and frames [22]. The skins and reinforcements were each constructed using stacks of dry warp-knit fabrics of Douglas Material Specification (DMS) 2436 Type 1, Class 72, Grade A carbon fiber that were stitched together using a 1200 denier VectranTM thread to form the skeleton of the skin-stiffened structure (preform) prior to DMS 2479 Type 2, Class1, VRM-34 epoxy resin infusion and cure [22, 23]. The cured panels were then coated with a white aerospace-grade waterborne dielectric primer/paint. NASA applied a white coating on PRSEUS panels to help visualize cracks or delamination that may occur during mechanical testing. Lee *et al.* [13] used two such PRSEUS panels to characterize the lightning damage resistance and tolerance of stitched composites, and the third panel was used in the current study.

In references [13, 24, 25], a series of lightning strike tests with nominal peak currents of 50, 125, and 200 kA were performed at four representative PRSEUS panel locations (*i.e.*, mid-bay, stringer, frame, and frame/stringer intersection). Nondestructive and destructive evaluation of the PRSEUS panel showed that through-thickness lightning-induced thermal damage was restricted to the outermost plies [25]. For example, cross-sectional microscopic inspection of two mid-bay locations subjected to 50 and 125 kA showed that damage only extended to the second and fifth ply, respectively [25]; the degree of through-thickness damage decreased sharply with radial distance from the arc channel axis. This makes sense since, for a given ply, the in-plane electrical conductivity in the fiber direction is substantially greater than the matrix-dominated through-thickness conductivity. In addition, there was no evidence of any damage near the innermost surface of the panel. These experimental results are consistent with those reported in the literature [18, 26-29]. In addition, Lee *et al.* [15] performed numerical simulations of 494 kA lightning strikes to 32-ply IM600/133 carbon/epoxy laminates that showed thermal damage development was restricted to the outermost 3–5 plies.

Figure 2 [24] shows typical lightning strike damage at a PRSEUS mid-bay location (*i.e.*, skin area between VectranTM stitch lines) subjected to a 124 kA peak current. The lightning-induced damage consisted of *i)* “primary” intense local damage (*i.e.*, combined large-scale matrix decomposition, fiber sublimation/ablation, fiber rupture, tow splitting, and delamination observed within the dashed blue ellipse in Fig. 2) occurring at the lightning attachment

point; and *ii*) “secondary” surrounding widespread surface damage (*i.e.*, small-scale fiber damage in the form of periodically dispersed tufts of broken fibers, and surface scorching/burning shown within the red ellipse in Fig. 2) occurring in the proximity but further from the intense damage zone. The primary intense local damage was mainly due to the direct lightning current conduction at the attachment point [13]. Essentially, the local composite temperature increased rapidly (due to Joule heating) as the lightning arc-core attached to the surface of a PRSEUS panel. As the epoxy matrix started to degrade, progressive evolution of volatile compounds, breakdown/depolymerization of the molecular chains, and char and residue formation occurred. As the local composite temperature increases, the carbon fibers will contract rapidly because of their negative CTE. This contraction, coupled with large CTE mismatches between the carbon fibers and epoxy matrix, can contribute to large-scale fiber breakage; this process can be exacerbated by high-temperature gradients in the composite. However, the widespread surface damage (Fig. 2) cannot be attributed to direct current injection since the primary conduction path occurs in the outer ply fiber direction. This diffuse widespread surface damage forms away from the lightning attachment point in a direction perpendicular to the fibers, as indicated by the yellow arrows in Fig. 2.

The lightning damage pattern observed in the mid-bay location of the PRSEUS panel (Fig. 2, [24]) prompts the question: what causes the formation of the widespread surface damage (*i.e.*, periodic distributions of tufts of broken fibers) found in the domain surrounding the area with intense local damage? Two potential causes of the widespread surface damage were investigated in this paper: *i*) magnetically-induced currents generated by a time-varying magnetic field, and *ii*) lightning arc-channel expansion over the struck surface.

2 Material and methods

2.1 PRSEUS concept

The PRSEUS panel fabrication process is distinct from that of traditional composite laminates. PRSEUS is a unitized out-of-autoclave co-cured structure with damage confinement features [30-33]. PRSEUS pre-assembly combines warp-knitted skin stacks, tear straps, frame caps, stringers, and frames with Vectran™ stitching threads [33]. These stitches impede delamination growth by arresting cracks and suppressing crack propagation [31, 32]. An exploded isometric view of a PRSEUS inner mold line (IML) side of a typical skin-stringer-frame interconnection is shown schematically in Fig. 3 [32, 33]. PRSEUS components (skin, stringer, frame, *etc.*) are made

of DMS 2436 Type 1, class 72, grade A, warp-knitted multi-axial AS4 carbon fiber fabrics infused with Hexcel's Hexflow DMS 2479 Type 2, Class 1, VRM-34 epoxy-resin [32]. The outer mold line (OML) skin is comprised of two 1.32 mm thick nine-ply stacks of dry warp-knitted AS4 unidirectional carbon fiber fabric. Each stack has a layup of [+45/-45/0₂/90/0₂/-45/+45] pre-knitted together with nylon-coated polyester threads. Stringers are composed of a single warp-knit stack that forms the flange/web and encloses the bulb, as illustrated in Fig. 3. Each stringer bulb is stiffened by inserting a pre-cured T800/3900-2B carbon-epoxy pultruded rod. Each sandwich-construction frame consists of a Rohacelle foam core [32], wrapped with a double warp-knit stack and stitched to the frame cap. Each frame contains multiple keyholes for the stringers to pass through. These elements are stitched together with 1200 denier Vectran™ threads to ensure residual load-carrying capabilities, improve bending stiffness, and suppress delamination between the skin stacks of a PRSEUS panel. For a typical Vectran™ stitch pattern, the stitching spacing and pitch are 25.4 mm and 5.1 mm [13], respectively. The dry carbon fiber fabric preform assembly is infused with Hexcel's Hexflow DMS 2479 Type 2, Class 1 VRM-34 resin using the Controlled Atmospheric Pressure Resin Infusion (CAPRI) process, and oven cured [32].

2.2 High impulse current generator setup and grounding conditions

The lightning strike testing was performed in the Mississippi State University (MSU) High Voltage Laboratory (HVL). The impulse current generator configuration (Fig. 4a) included *i*) eight high-voltage capacitors each capable of storing 50 kJ of electrical energy (Fig. 4b); *ii*) eight 1 kΩ resistors (Fig. 4b); *iii*) a 9 cm in diameter hemispherical brass output electrode (Fig. 4b) to induce the lightning arc discharge; and *iv*) a trigatron (Fig. 4c) to trigger the current discharge from the capacitors through the resistors to the output electrode. The electrical circuit was arranged to produce a modified standard impulse waveform component A in compliance with the Society of Automotive Engineers (SAE) Aerospace Recommended Practice (ARP) 5412 [34]. The nominal values of the current waveform parameters used in this study included *i*) a rise time of 6.4 μs ±20% tolerance (*i.e.*, the time required for the electrical current to rise from 10% to 90% of the peak amplitude), *ii*) a decay time of 69 μs (*i.e.*, the time necessary for the electrical current to decrease to half the peak amplitude), and *iii*) an action integral of $2 \times 10^5 A^2s$ (*i.e.*, the time integral of the joule heating power).

The generator was centrally located inside a steel frame, as shown in Fig. 4a. A vertically oriented polyvinyl chloride (PVC) pipe was used to enclose the generator's output electrode and physically support the PRSEUS panel.

The 9 cm diameter hemispherical electrode minimizes field enhancement while ensuring a localized arc attachment at or near the central axis of the electrode since this is the shortest distance to the infinite parallel plane (*i.e.*, the OML surface of the PRSEUS panel). The gap distance between the output electrode and the PRSEUS panel was varied from 8.9 to 25.4 mm for desired nominal peak currents in the range of 50 to 200 kA [24, 25, 35]. In general, higher peak currents require larger air gaps to prevent self-triggering (electrical breakdown). The required voltage to charge the capacitors was a function of the desired peak current level. For instance, a 125 kA peak current strike required a charging voltage of 14 kV. Triggering the trigatron (Fig. 4c) initiated the capacitors' discharge through the resistors to the output electrode. Once the intensity of the electric field exceeds the dielectric strength of the air gap (*i.e.*, 3 kV/mm at standard atmospheric conditions), air molecules become ionized, which allow the flow of current, resulting in a local lightning arc attachment on the panel.

For electrical grounding purposes, the lateral edges along the perimeter of the PRSEUS panel were sanded to remove the insulating paint/epoxy-matrix and expose the conductive carbon fibers. This forced the current to flow in-plane and exit out of the panel. Braided copper wires were placed on top of the sanded area and secured on the panel edges with aluminum angle strips using C-clamps, as shown in Fig. 4d. To dissipate the lightning strike current, each aluminum strip was bolted to another braided wire that was connected to the grounded steel frame surrounding the generator.

2.3 PRSEUS panel lightning strike test matrix

In this paper, the PRSEUS panel OML skin was modified to include various insulating barriers to investigate lightning-induced surface damage for cases where the anisotropic lightning arc-root/channel expansion and/or the lightning arc primary current were limited or constrained by these barriers. The barriers included through-slots (*i.e.*, rectangular-shaped openings through the skin of PRSEUS leaving an air gap in the structure), a through-slot filled with non-conductive silicon paste, insulating tape, and acrylic plates. Figure 5 shows the IML and OML sides of the pristine PRSEUS panel, respectively. The IML view (Fig. 5a) shows the stringer, frame, and mid-bay locations. The OML view (Fig. 5b) shows a map of intended lightning strike locations represented with yellow "x" marks near the symbolic insulating boundaries. The solid and dashed blue lines in the figure represent through-the-thickness Vectran™ chain stitch pattern locations.

To determine if lightning-induced magnetic currents or lightning arc-channel expansion is responsible for widespread surface damage (*cf.*, Fig. 2), the PRSEUS OML skin was modified as follows: A series of through-slots (18 cm long with an air gap width of 0.5 cm) were machined at several mid-bay locations between frames and stringers as shown on the left-hand side (LHS) of Fig. 5b. Three slots were machined parallel to the fibers in the outermost +45° ply, and three other slots were machined perpendicular to this fiber direction. The center of each unfilled through-slot was located roughly 4 cm from the desired lightning strike attachment point. The purpose of the machined slots was to prevent primary currents (*i.e.*, lightning arc direct current injection) from flowing across the slot. Hence, any damage that forms on the side of the composite opposite to the lightning arc attachment point must be due to some mechanism besides primary direct current injection (*i.e.*, magnetically-induced current or lightning arc-channel expansion).

In addition, a variety of different non-conductive surface modifications were made to the PRSEUS OML skin adjacent to (or surrounding) the intended lightning attachment points, as shown on the right-hand side (RHS) of Fig. 5b. *First*, a 0.6 cm × 30.5 cm ($W \times L$) horizontal slot (oriented parallel to the 0° fibers) was machined in the upper right mid-bay location, where the slot was located roughly 2.5 cm from the desired lightning strike attachment point. The slot was filled with a high dielectric strength silicon paste “Molykote™ 4 electrical insulating compound” with an electrical resistivity of $1.1 \times 10^{15} \Omega\text{cm}$ [36] that was greater than that of air $10^{12} \Omega\text{cm}$ [37].

Second, several layers of 2 cm wide and 0.025 cm thick electrically non-conductive “Scotch® heavy-duty vinyl electrical tape” with an electrical resistivity of $1 \times 10^{12} \Omega\text{cm}$ [38] were used to bound three 5 cm × 6 cm ($W \times L$) rectangular areas centered about three mid-bay lightning strike locations, as indicated on the RHS of Fig. 5b. The area enclosed by the insulating tape (30 cm²) was far less than the widespread surface damage area (205 cm² [24]) produced by a typical 125 kA nominal peak current lightning strike to an unmodified PRSEUS mid-bay skin (*cf.*, Fig. 2; [24]). Hence, the insulating tape can be used to observe the nature and extent of lightning damage in a confined area near the attachment point, as well over a broader surrounding area with a greater surface resistivity.

Lastly, 0.5 cm thick insulating acrylic sheets (resistivity, $1 \times 10^{16} \Omega\text{cm}$ [39]) were placed at OML mid-bay locations near the lightning strike attachment points, as illustrated in Fig. 5b. Three different acrylic plate configurations were considered: 1) A pair of parallel 10 cm × 20 cm ($W \times L$) plates, separated by 6 cm, were located symmetrically about the anticipated lightning strike location, and oriented perpendicular to the outer ply fiber direction. 2) A single

10 cm × 20 cm ($W \times L$) plate was orientated vertically (*i.e.*, at 45° to the outer ply fiber direction) at a nominal 3 cm distance from the planned lightning strike locations. 3) A 21 cm × 21 cm ($W \times L$) square plate with a 9 cm diameter hole was centered about the nominal lightning strike location. Unlike the adhesive insulating tape, the acrylic plates were simply arranged and placed between the PVC pipe and the OML surface of the PRSEUS panel with no bonding agent. The weight of the upside-down panel held the acrylic plates in place. Similar to the filled slot and insulating tape, the acrylic sheets can be used to assess lightning damage development in regions with non-uniform through-thickness or surface resistivities.

The electrical resistivities for *i*) the non-conductive silicon used to fill the horizontal through-slot ($1.1 \times 10^{15} \Omega\text{cm}$), *ii*) insulating tape ($1 \times 10^{12} \Omega\text{cm}$), and *iii*) acrylic plates ($1 \times 10^{16} \Omega\text{cm}$) were all substantially larger than those for typical carbon-epoxy composites ($2.5\text{--}15 \times 10^{-5} \Omega\text{cm}$ [3-5]). These surface modifications would likely have little effect on the primary intense local damage occurring at the lightning attachment point but could significantly disrupt the formation of secondary widespread surface damage (*cf.*, Fig. 2). If the extent and severity of widespread surface damage was inhibited by the presence of insulating barriers, then such damage is likely attributable to arc-expansion. These insulating barriers, however, would not prevent the arc channel's magnetic fields from inducing secondary currents (magnetically-induced currents) in conductive fibers beyond (or underneath) the barrier boundaries. Thus, if widespread surface damage developed in the modified PRSEUS panel across or underneath insulating boundaries, then magnetically-induced currents in the outer area surrounding the arc attachment point would arguably be responsible for secondary lightning damage formation.

3 Results and discussion

The modified PRSEUS panel was subjected to a series of nominal 50 kA and 125 kA OML mid-bay strikes. A total of 15 strikes were performed: *i*) three strikes adjacent to unfilled through-slots oriented *parallel* to the outermost ply fiber direction (+45°); *ii*) three other strikes near unfilled through-slots oriented *perpendicular* to the outermost fiber direction; *iii*) two strikes near a horizontal slot filled with a non-conductive silicon paste; *iv*) one strike to each of the three 5 cm × 6 cm rectangular areas bounded by non-conductive tape; and *v*) four strikes bounded on one or more sides by overlaid non-conductive acrylic plates. Table 1 summarizes the lightning strike tests performed on a PRSEUS panel modified to include the non-conductive barriers.

Table 1. Lightning strike tests performed on a PRSEUS OML mid-bay locations modified to include non-conductive barriers.

Non-conductive barriers	Dimensions (cm)	Number of tests	Peak currents (kA)
Slot parallel to the +45° fiber direction	$0.5W \times 18L \times 0.26T$	3	118.4
			120.0
			136.0
Slot perpendicular to the +45° fiber direction	$0.5W \times 18L \times 0.26T$	3	53.0
			117.0
			120.0
Slot filled with insulating silicon paste ^a	$0.6W \times 30.5L \times 0.26T$	2	58.0
			100.4
Electrically insulating tape ^b	$2W \times 0.025T$	3	116.0
			116.0
			126.0
One insulating acrylic plate	$10W \times 20L \times 0.5T$	2	124.4
			126.0
Two insulating acrylic plates	$10W \times 20L \times 0.5T$	1	44.4
Insulating acrylic plate with a 9 cm-diameter circular hole	$21W \times 21L \times 0.5T$	1	53.2

^aMolykote™ 4 electrical insulating compound [36]

^bScotch® heavy-duty vinyl electrical tape [38]

^cAcrylic sheets [39]

Lightning strike damage to the modified PRSEUS panel included intense local damage formed immediately at the strike location: large-scale broken carbon fibers protruding from the OML surface accompanied by extensive matrix decomposition, combustion, and vaporization. Severe damage in this region tended to elongate in the outer ply fiber direction (+45°) at the lightning attachment point, while the widespread surface damage (*i.e.*, tufts of broken fibers) tend to mainly spread *perpendicular* to the fiber direction, consistent with results reported in references [13, 20, 21, 24, 25] and shown in Fig. 2. The presence of nearby insulating barriers, however, did limit the formation and extent of lightning-induced surface damage, as discussed in the following subsections. Since the primary focus of this work is to determine the mechanisms behind widespread surface damage formation, no destructive sectioning of the modified PRSEUS panel was performed. As mentioned previously, 50–125 kA lightning strikes to a similar PRSEUS panel resulted in local through-thickness damage to the outermost 2–5 plies [25].

3.1 Effect of adjacent unfilled through slots parallel to the outermost fiber direction on surface damage formation

The modified PRSEUS panel (Fig. 5) was subjected to three nominal 125 kA OML mid-bay strikes, where the intended arc attachment points were located approximately 4 cm from unfilled through slots ($0.5 \text{ cm } W \times 18 \text{ cm } L \times 0.26 \text{ cm } T$) oriented parallel to the +45° outer ply fiber direction, as shown in Fig. 6. In the figure, the yellow “x” mark indicates the approximate initial arc attachment point. In general, this point must fall

within a radial distance of the central axis of the output electrode that is a small fraction of the given air gap length (Fig. 6a). Since no electrical current can flow across the air gap within the slot (and the primary electrical conduction path is along the carbon fibers), any damage that forms on the opposite side of the slot from the attachment point cannot be due to direct lightning current. Consistent with [13, 24, 25], the lightning damage included a primary intense local damage area (*i.e.*, severe fiber rupture, matrix decomposition, delamination, chipped paint, surface scorching) surrounded by a distributed cluster of tiny broken fibers and longitudinal strips of split fibers. Unlike the cases involving strikes to unmodified PRSEUS mid-bay locations [13, 24, 25] (*cf.*, Fig. 2), lightning damage to PRSEUS panel with parallel through slots was not symmetric about the attachment point (Fig. 6). The presence of the slot limited the spread of the primary intense surface damage as well as the formation of widespread damage.

Figures 6a-b show lightning damage due to an actual 120 kA mid-bay strike, where the slot was oriented parallel to the outer ply fiber direction (+45°). Similar to the results shown in Fig. 2, a region of intense local damage formed at the attachment point and was elongated in the outer ply fiber direction. In addition, widespread surface damage formed on both sides of the slot (Fig. 6b) but was less pronounced on the isolated side of the slot. This distributed damage tended to be loosely clustered about an axis perpendicular to the fiber direction that also passed through the attachment point. This axis roughly defines the direction of maximum arc expansion [20], as well as the location of the peak magnetically-induced currents [25, 35, 40]. In this experiment, it is unclear whether the surface damage occurring on the opposite side of the unfilled slot resulted from reattachment of the expanding arc (which “jumped” the slot due to the presence of high electric field) or from the formation of strong secondary currents induced by the primary magnetic field. This was the only experiment, however, where damage formed on the opposite side of an unfilled slot.

Additional strikes at 118.4 kA (Fig. 6c) and 136 kA (Fig. 6d) were performed adjacent to parallel slots at mid-bay locations. In each case, the domain with intense fiber damage was more rectangular-shaped and noticeably more pronounced than for the earlier 120 kA strike (Fig. 6b). Moreover, in these latter two cases, *no widespread surface damage appeared across the slot from the attachment point*. It seems reasonable that the discontinuity in surface geometry provided by the slot caused the expanding arc to detach from the surface, leading to more pronounced

damage on the strike side of the slot. In addition, any magnetically-induced currents were insufficient to produce damage across the slot (the magnetic field decays with radial distance from the arc core [41]).

3.2 *Effect of adjacent unfilled through slots perpendicular to the outermost fiber direction on surface damage formation*

Three lightning strike tests were performed at mid-bay locations on the modified PRSEUS panel where the intended arc attachment points were located approximately 4 cm from unfilled through-slots (0.5 cm W × 18 cm L × 0.26 cm T) *perpendicular* to the +45° outer ply fiber direction (*i.e.*, the primary electrical conduction path was orthogonal to the slot). Figures 7a-c show lightning damage adjacent to perpendicular slots for measured lightning peak currents of 53 kA, 117 kA, and 120 kA, respectively. In all three tests, *no visible lightning damage formed on the opposite side of the unfilled slot* from the attachment point. This makes sense since the air-gap within the slot prevents the flow of high electrical current injected at the lightning attachment point from spanning the slot. In addition, the geometric discontinuity due to the slot likely caused the expanding arc to detach from the surface resulting in no damage across the slot (and proportionally more damage on the strike side of the slot). As an aside, the disruption in the primary current due to the slot will undoubtedly affect the formation of magnetically-induced currents adjacent to the attachment point.

The central regions with intense local damage appeared more rectangular-shaped, with clear evidence of spallation of outer ply material at the edge of the slot (Fig. 7a-c). This is similar to lightning strike damage observed adjacent to unfilled parallel slots (*cf.*, Fig. 6c-d). The damage was not symmetric about the axis perpendicular to the +45° outer ply fiber direction passing through the attachment point due to the presence of a perpendicular slot. In addition, a number of ribbon-like strips with severe fiber damage and/or spallation formed parallel to the fiber direction at and near the slots; these strips were located somewhat outside the typical regions with intense damage. Such ribbon-like regions with acute fiber/surface damage were not widely observed in previous lightning strike experiments performed on unmodified PRSEUS panels [13, 24, 25]. Moreover, no large-scale widespread surface damage (periodically distributed tufts of broken fibers) appeared in the OML skin of the slotted panel (Fig. 7). The results support the assumption that the non-conductive barriers disrupt damage formation on the panel.

The presence of a slot appears to alter the arc root-shape, attachment, expansion, as well as the distribution of local primary electrical currents, magnetically-induced currents, Joule heating, and other factors contributing to composite lightning damage formation. For an unbounded PRSEUS panel subjected to lightning strike, severe damage will generally form in an elliptical domain symmetrically located about the attachment point, where the semi-major radius of the ellipse is aligned with the primary conduction path (Fig. 2). For panels with orthogonal slots, the primary conduction path is severed on one side of the attachment point. This likely leads to increased local Joule heating at the attachment point near the slot, which may explain proportionally more matrix decomposition, acute fiber ruptures, and/or spallation occurring near the slot. The slot may also result in forced electrical current flow *perpendicular* to the fiber direction (that subsequently gets conducted away from the slot in parallel fiber tows) and/or strong magnetically-induced currents that drive the formation of ribbon-like regions with acute fiber/surface damage rather than distributed surface damage. Also, arc expansion will be more pronounced perpendicular to the outer ply fibers (*i.e.*, parallel to the slot), which may contribute to the spread of surface damage.

3.3 *Effect of an insulated filled slot on surface damage formation*

Two lightning strike tests were performed at mid-bay locations on the modified PRSEUS panel, where the intended arc attachment points were located approximately 2.5 cm below a horizontal non-conductive (silicon paste) filled slot (0.6 cm $W \times$ 30.5 cm $L \times$ 0.26 cm T) oriented parallel to the 0° fibers. The purpose of this experiment was to evaluate if the lightning damage would form across from the filled slot in the absence of the primary current conduction path (*i.e.*, carbon fibers). Figures 8a-b show the induced lightning strike damage adjacent to a filled slot for applied current levels of 58.0 and 100.4 kA, respectively. The red rectangles in the figure represent the locations of the filled slot. The dashed blue lines in Fig. 8 represent the location of through-thickness Vectran™ stitches. Both strikes exhibited severe lightning damage (*i.e.*, matrix decomposition, fiber breakage, delamination) accompanied by adjacent parallel strips (along the +45° fiber direction) with large-scale fiber rupture. Not surprisingly, the damaged area was less severe for the 58.0 kA strike (Fig. 8a) than the 100.4 kA strike (Fig. 8b). Since the degree of Joule heating is proportional to the electrical energy (which is also proportional to the square of the applied electrical current “action integral”), higher peak current leads to markedly more significant lightning damage.

The presence of the filled slot appeared to limit the spread of the primary intense local damage. In contrast to the case for unfilled perpendicular slots (Fig. 7), however, *damage formed on both sides of the slot*. For example, the

100.4 kA strike (Fig. 8b) induced parallel strips with severe fiber breakage on both sides of the filled slot. A solid insulator (*e.g.*, silicon) can become conductive under extreme conditions such as a massive current flow or an external electric field. Its change in electrical conductivity is typically followed by irreversible deformation. Careful inspection near the attachment points in Fig. 8 showed that the silicon paste within the slot was relatively undeformed, except for slight surface scorching due to excessive heating. This suggests that there was little to no current flow through the filled slot, and surface damage on the isolated side of the slot resulted from arc expansion. Since there was no *geometric* discontinuity in the PRSEUS OML surface, it is possible that the expanding arc remained attached or reattached after traversing the filled slot.

3.4 Effect of an insulating tape on surface damage formation

The modified PRSEUS panel (Fig. 5) was subjected to three nominal 125 kA OML mid-bay strikes. The intended arc attachment points were each located at the center of a 5 cm \times 6 cm ($W \times L$) open rectangular area bounded by several layers of electrically insulating tape (2 cm $W \times$ 0.025 cm T). This surface treatment was applied to limit the lightning arc-root/channel expansion (and current injection) in a confined area of 30 cm² without affecting the induced magnetic fields and the primary current flow through the conductive fibers. In comparison, a typical unconstrained 124 kA mid-bay strike (*cf.*, Fig. 2) would result in an elliptical surface damage with a total area of 205 cm². Thus, if the surface damage is due to the magnetically-induced current, widespread surface damage should form underneath or beyond the tape barrier.

Figures 9a-c show lightning damage within the enclosed area for measured lightning peak currents of 116.0, 116.0, and 126.0 kA, respectively. The symbolic tape boundaries in the figure are not scaled. Consistent with results reported in references [13, 24, 25] and shown in Fig. 2, the two 116.0 kA strikes (Fig. 9a-b) resulted in intense local damage at the attachment point accompanied by surrounding tufts of broken fibers. While the intended strike location was the center of the rectangle, the actual lightning attachment point was somewhat off-center. The complex plasma physics, spherical output electrode geometry, and finite gap distance make it difficult to precisely control the trajectory of the lightning arc discharge. Careful inspection of the inner edges of the non-conductive tape showed minor scorching surrounding the exposed PRSEUS OML surface with intense fiber damage. Additionally, the 126.0 kA strike (Fig. 9c) resulted in more severe localized damage (*i.e.*, matrix decomposition/pyrolysis, fiber rupture, and delamination) that extended all over the uncovered rectangular area; the inner edges of the non-

conductive tape were partially melted/burned. As previously discussed, higher peak current leads to more Joule heating resulting in significant lightning damage.

Remarkably, *no widespread surface damage occurred under or across the non-conductive tape boundary* for all the three strikes (Fig. 9). In each case, the visible surface damage was completely confined to the 5 cm × 6 cm open area; except for some minor surface scarfing mostly around the perimeter of the intense fiber damage area. These experiments confirm that the widespread surface damage in a PRSEUS panel must be a result of an expanding lightning arc-root/channel upon attachment to the surface of the composite. The insulating tape prevented significant current injection from the expanding arc into the underlying skin. In addition, the slight step discontinuity in OML surface geometry due to the tape may cause the expanding arc to detach.

3.5 Effect of insulating acrylic plates on surface damage formation

To further probe the effect of surface treatments on lightning damage development, additional mid-bay strikes were performed where 0.5 cm thick insulating acrylic plates were placed on the OML surface to limit the arc expansion in different directions without affecting the induced magnetic fields. Four lightning strike tests were performed on modified PRSEUS OML mid-bay locations adjacent to overlaid insulating acrylic plates positioned in different orientations with respect to the outermost ply fiber direction. One 44.4 kA strike was centered between two separated sheets of parallel acrylic plates (with a spacing of 6 cm) oriented perpendicular to the fiber direction (Fig. 10a). Two strikes (124.4 and 126.0 kA) were performed adjacent to an acrylic plate oriented 45° to the outermost ply fiber direction (Fig. 10b-c). Finally, a 53.2 kA strike was carried at the center of a square acrylic plate with a 9 cm diameter hole (Fig. 10d). The symbolic acrylic plate boundaries in the figure are not scaled. The dashed blue lines in Fig. 10 represent the location of through-thickness Vectran™ stitches. The lightning strike damage consisted of an intense localized fiber damage area at the attachment point surrounded by widespread surface damage. Consistent with results reported in [13, 25], Vectran™ stitches remained intact and locally constrained surface damage formation.

In each of the performed lightning strike tests, *no visible surface damage formed across and/or beneath the insulating acrylic plate boundaries*. For instance, in Fig. 10a, the placement of the two (10 cm W × 20 cm L × 0.5 cm T) acrylic plates 3 cm above and 3 cm below the intended strike location,

respectively, limited the intense local damage along the fiber axis. The widespread surface damage, however, expanded normal to the outermost ply fiber direction on the unconstrained sides, which correspond to the direction of a rapid arc expansion [20]. Similarly, the lightning damage due to the 124.4 and 126.0 kA peak current strikes (Fig. 10b-c) was constrained by the adjacent vertically orientated (10 cm $W \times 20$ cm $L \times 0.5$ cm T) acrylic plates. The lightning surface damage extended in the fiber direction right up to the insulating acrylic plate but did not cross the acrylic barriers. The acrylic plate boundaries (oriented 45° and 90° to the fiber direction as shown in Fig. 10a-c) prohibited continued arc expansion/attachment along the fiber direction, forcing the surface damage to expand in unconstrained directions and parallel to the acrylic barrier edges.

In addition, a 53.2 kA mid-bay strike was conducted at the center of a (21 cm $W \times 21$ cm $L \times 0.5$ cm T) square acrylic plate with a 9 cm diameter circular cut out (Fig. 10d). Consistent with the non-conductive tape experiment results (Fig. 9), the lightning damage was completely confined in the open circular cut-out area of 64 cm². For comparison, a typical surface damage area of an unconstrained mid-bay strike subjected to a nominal peak current of 50 kA is 96 cm² [24]. The damage consisted of a relatively smaller intense local damage area at the attachment point surrounded by tufts of broken fibers that were limited by the acrylic plate boundary.

The insulating properties of the acrylic plates coupled with the 0.5 cm step discontinuity in surface geometry at the plate boundaries clearly altered the interaction between the expanding arc and the surface, which influenced the shape of the surface damage. The acrylic sheets, however, would not influence the magnetically-induced currents. These results confirm that lightning arc-root/channel expansion is responsible for widespread surface damage formation on a PRSEUS panel.

4 Conclusions

Lightning strike to a carbon-epoxy PRSEUS composite panel results in *i*) a primary intense localized fiber damage area at the attachment point and *ii*) widespread surface damage in the proximity but further from the intense damage zone. This paper focused on determining the causes of widespread distributed surface damage. Such damage cannot be attributed to direct lightning current injection since the primary conduction path is in the outer ply fiber direction, and widespread surface damage forms orthogonal to that direction. Two primary driving mechanisms were thoroughly investigated: *i*) magnetically-induced currents and *ii*) lightning arc-root/channel expansion.

To probe which of the two mechanisms is responsible for widespread surface damage formation, a series of nominal 50 and 125 kA simulated lightning strike tests were performed on a PRSEUS panel, where the outer mold line (OML) mid-bay surface was modified to include machined through-slots, a non-conductive silicon-filled slot, electrically insulating tape, and acrylic plates. These barriers were placed adjacent to, or enclosing, the intended arc attachment points to investigate the effect of such insulating boundaries on lightning damage formation without influencing or restricting the development of magnetically-induced currents. The machined through-slots and the silicon-filled slot severed the primary current conduction path, whereas the externally applied insulating tape and the acrylic plates restricted or confined the lightning arc expansion and attachment.

Simulated lightning strike testing showed that the lightning-induced surface damage region was completely confined within the boundary formed by externally applied insulating surface treatments (*i.e.*, insulating tape, and acrylic plates); no damage formed beyond (or underneath) these barriers. Since such non-conductive layers do not influence the generation of magnetically-induced currents, then any changes in surface damage formation must be due to lightning arc-root/channel expansion. The presence of unfilled through-slots adjacent to the lightning arc attachment point generally prevented damage formation across the slots. In contrast, significant lightning surface damage formed on the isolated side of the silicon-filled slot. This suggests that physical discontinuities in the OML surface geometry may influence the lightning arc-root shape, attachment, expansion, and other factors that govern the interaction between the expanding arc and the panel surface.

These experimental results demonstrated that lightning arc-root/channel expansion is the primary driving factor in the formation of widespread surface damage. This paper can motivate novel lightning strike protection techniques that prevent the arc from attaching to the surface of a composite or constraining the arc in a confined area where it can be quickly dissipated. Lastly, the effect of minor step discontinuities in OML surface geometries on lightning arc expansion, current injection, and damage formation remains to be fully investigated.

5 Acknowledgments

This study was performed at Mississippi State University (MSU) and funded by the Boeing Company (contract number 1188469). The authors would like to express their sincere gratitude to the Marvin B. Dow Stitched

Composites Development Center, the High Voltage Laboratory (HVL) operators at MSU, and Patrick Trash (Boeing, Huntington Beach, CA) for their support.

6 References

- [1] Rupke E. Lightning direct effects handbook. Pittsfield, MA: Lightning Technologies Inc.; 2002.
- [2] Fisher FA, Plumer JA. Lightning protection of aircraft. National Aeronautics and Space Administration; 1977. p. 560.
- [3] Reid GW. Mechanical damage to aircraft structures from lightning strikes. Proceedings of the Institution of Mechanical Engineers, Part G: Journal of Aerospace Engineering. 2016;207(1):1-14.
- [4] Luo X, Chung DDL. Electromagnetic interference shielding using continuous carbon-fiber carbon-matrix and polymer-matrix composites. Composites Part B: Engineering. 1999;30(3):227-31.
- [5] Park J, Lee S, Choi J. Cure monitoring and residual stress sensing of single-carbon fiber reinforced epoxy composites using electrical resistivity measurement. Composites Science and Technology. 2005;65(3-4):571-80.
- [6] Lee J, Lacy TE, Pittman CU, Mazzola MS. Thermal response of carbon fiber epoxy laminates with metallic and nonmetallic protection layers to simulated lightning currents. Polymer Composites. 2018;39(S4):E2149-E66.
- [7] Lee J, Lacy Jr. TE, Pittman Jr. CU, Mazzola MS. Temperature-dependent thermal decomposition of carbon/epoxy laminates subjected to simulated lightning currents. Polymer Composites. 2018;39(S4):E2185-E98.
- [8] Feraboli P, Miller M. Damage resistance and tolerance of carbon/epoxy composite coupons subjected to simulated lightning strike. Composites Part A: Applied Science and Manufacturing. 2009;40(6-7):954-67.
- [9] Chemartin L, Lalande P, Peyrou B, Chazottes A, Elias PQ, Delalondre C, Cheron BG, Lago F. Direct effects of lightning on aircraft structure: Analysis of the thermal, electrical and mechanical constraints. Aerospace Lab. 2012(5):p. 1-15.
- [10] Savvatimskiy AI. Measurements of the melting point of graphite and the properties of liquid carbon (a review for 1963–2003). Carbon. 2005;43(6):1115-42.
- [11] Kim HS, Shioya M, Takaku A. Sublimation and deposition of carbon during internal resistance heating of carbon fibers. Journal of Materials Science. 1999;34(18):4613-22.
- [12] Morgan D, Hardwick CJ, Haigh SJ, Meakins AJ. The interaction of lightning with aircraft and the challenges of lightning testing. AerospaceLab. 2012(5):1-10.
- [13] Lee J, Gharghabi P, Boushab D, Ricks TM, Lacy TE, Pittman CU, Mazzola MS, Velicki A. Artificial lightning strike tests on PRSEUS panels. Composites Part B: Engineering. 2018;154:467-77.
- [14] Lee J, Lacy TE, Pittman CU. Lightning mechanical damage prediction in carbon/epoxy laminates using equivalent air blast overpressure. Composites Part B: Engineering. 2021;212:108649.
- [15] Lee J, Lacy TE, Pittman CU, Reddy JN. Numerical estimations of lightning-induced mechanical damage in carbon/epoxy composites using shock wave overpressure and equivalent air blast overpressure. Composite Structures. 2019;224:111039.
- [16] Wang F, Ma X, Chen H, Zhang Y. Evolution simulation of lightning discharge based on a magnetohydrodynamics method. Plasma Science and Technology. 2018;20(7):075301.
- [17] Larsson A, Lalande P, Bondiou-Clergerie A, Lalande P, Delannoy A. The lightning swept stroke along an aircraft in flight. Part I: thermodynamic and electric properties of lightning arc channels. Journal of Physics D: Applied Physics. 2000;33(15):1866-75.
- [18] Lago F, Gonzalez JJ, Freton P, Uhlig F, Lucius N, Piau GP. A numerical modelling of an electric arc and its interaction with the anode: part III. Application to the interaction of a lightning strike and an aircraft in flight. Journal of Physics D: Applied Physics. 2006;39(10):2294-310.
- [19] Herziger G, Bakowsky L, Peschko W, Lindner FW. Dynamics of radial arc expansion. Physics Letters A. 1978;69(4):273-5.
- [20] Martins RS. Experimental and theoretical studies of lightning arcs and their interaction with aeronautical materials: UNIVERSITE PARIS-SACLAY; 2016.
- [21] Kawakami H. Lightning strike induced damage mechanisms of carbon fiber composites: University of Washington; 2011.
- [22] Velicki A, Hoffman K, Linton KA, Baraja J, Wu H-YT, Thrash P. Hybrid wing body multi-bay test article analysis and assembly final report. 2017.

- [23] Velicki A, Yovanof N, Baraja J, Linton K, Li V, Hawley A, Thrash P, DeCoux S, Pickell R. Damage arresting composites for shaped vehicles–Phase II final report. 2011.
- [24] Boushab D. Lightning damage resistance of a full-scale flat PRSEUS panel: Mississippi State University; 2020.
- [25] Lacy T, Mazzola M, Kluss J, Boushab D, Gharghabi P, Lee J, Ricks T, Aniket M, Khari H. Resin infused stitched composite development final report: Lightning strike testing on PRSEUS panels. Boeing Technical Report 2018.
- [26] Hirano Y, Katsumata S, Iwahori Y, Todoroki A. Artificial lightning testing on graphite/epoxy composite laminate. *Composites Part A: Applied Science and Manufacturing*. 2010;41(10):1461-70.
- [27] Kamiyama S, Hirano Y, Ogasawara T. Delamination analysis of CFRP laminates exposed to lightning strike considering cooling process. *Composite Structures*. 2018;196:55-62.
- [28] Li Y, Li R, Lu L, Huang X. Experimental study of damage characteristics of carbon woven fabric/epoxy laminates subjected to lightning strike. *Composites Part A: Applied Science and Manufacturing*. 2015;79:164-75.
- [29] Wolfrum J, Schuster TJ, Körwien T. Effects of heavy lightning strikes on pristine and repaired carbon composite structures. *Journal of Composite Materials*. 2017;51(25):3491-504.
- [30] Bergan A, Bakuckas Jr JG, Lovejoy A, Jegley D, Linton K, Neal B, Korkosz G, Awerbuch J, Tan T-M. Full-scale test and analysis results of a PRSEUS fuselage panel to assess damage containment features. In: *Proceedings of Aircraft Airworthiness & Sustainment*. Baltimore, Maryland, Conference, Conference 2012.
- [31] Jegley DC. Experimental behavior of fatigued single stiffener PRSEUS specimens. 2009.
- [32] Velicki A, Hoffman K, Linton KA, Baraja J, Wu H-YT, Thrash P. Hybrid wing body multi-bay test article analysis and assembly final report. 2017.
- [33] Velicki A, Jegley DC. PRSEUS structural concept development. 52nd Aerospace Sciences Meeting 2014. p. 2014-0259.
- [34] Engineers SoA. Aircraft lightning environment and related test waveforms. *Aerospace Recommended Practice ARP 5412*: SAE International; 1999. p. 53.
- [35] Gharghabi P. Experimental and numerical studies of lightning strike induced damage to carbon fiber epoxy composites: Mississippi State University; 2020.
- [36] MOLYKOTE® 4 Electrical Insulating Compound. 2018.
- [37] Pawar SD, Murugavel P, Lal DM. Effect of relative humidity and sea level pressure on electrical conductivity of air over Indian Ocean. *Journal of Geophysical Research: Atmospheres*. 2009;114(D2).
- [38] Scotch® Vinyl Electrical Tape 22, 3/4 in x 36 yd, Black, 12 rolls/carton, 48 rolls/Case | 3M United States. 2015.
- [39] Physical properties of acrylite® FF. Parsippany, New Jersey: CYRO Industries; 2001.
- [40] Tholin F, Chemartin L, Lalande P. Simulation of the lightning arc root interaction with anisotropic materials. In: *Proceedings of ICOLSE 2017*. NAGOYA, Japan, Conference 2017-09-13, Conference 2017.
- [41] Wang B, Zhu Y, Ming Y, Yao X, Tian X, Ziegmann G, Duan Y, Sun J. Understanding lightning strike induced damage mechanism of carbon fiber reinforced polymer composites: An experimental study. *Materials & Design*. 2020;192:108724.

List of figures:

Fig. 1. Arc-root expansion of a 100 kA strike with respect to time upon attaching to the surface of (a) unpainted aluminum panel (b) painted aluminum panel (c) carbon-epoxy composite along the fiber direction (d) carbon-epoxy composite along the transverse direction. Adapted from [20]

Fig. 2. Typical lightning-induced damage at a PRSEUS panel mid-bay location subjected to 124 kA peak current level. Adapted from [24]

Fig. 3. Exploded view of a PRSEUS IML side preform assembly. Adapted from [32]

Fig. 4. (a) Impulse current generator setup, (b) top isometric view of the electrical components, (c) trigatron, and (d) electrical grounding condition of the PRSEUS panel.

Fig. 5. (a) IML, and (b) OML side views of a pristine PRSEUS panel with a schematic of the intended lightning strike locations near the insulating boundaries.

Fig. 6. Lightning strike damage adjacent to unfilled through slots oriented parallel to the outermost ply fiber direction due to peak currents of (a) 120 kA typical strike test setup, (b) 120 kA, (c) 118.4 kA, and (d) 136 kA.

Fig. 7. Lightning strike damage adjacent to unfilled through slots oriented perpendicular to the outermost ply fiber direction due to peak currents of (a) 53.0 kA, (b) 117.0 kA, and (c) 120.0 kA.

Fig. 8. Lightning strike damage adjacent to a horizontal slot parallel to the 0° fibers filled with non-conductive silicon paste due to peak currents of (a) 58.0 kA, and (b) 100.4 kA.

Fig. 9. Lightning strike damage at three mid-bay locations bounded by a non-conductive tape due to peak current levels of (a) 116 kA, (b) 116 kA, and (c) 126.0 kA.

Fig. 10. Lightning strike damage to four mid-bay locations bounded by insulating acrylic plates positioned in different orientations with respect to the outermost ply fiber direction due to peak current levels of (a) 44.4 kA, (b) 124.4 kA, (c) 126.0 kA, and (d) 53.2 kA.

List of tables:

Table 1. Lightning strike tests performed on a PRSEUS OML mid-bay locations modified to include non-conductive barriers.

Fig. 1. Arc-root expansion of a 100 kA strike with respect to time upon attaching to the surface of (a) unpainted aluminum panel (b) painted aluminum panel (c) carbon-epoxy composite along the fiber direction (d) carbon-epoxy composite along the transverse direction. Adapted from [20]

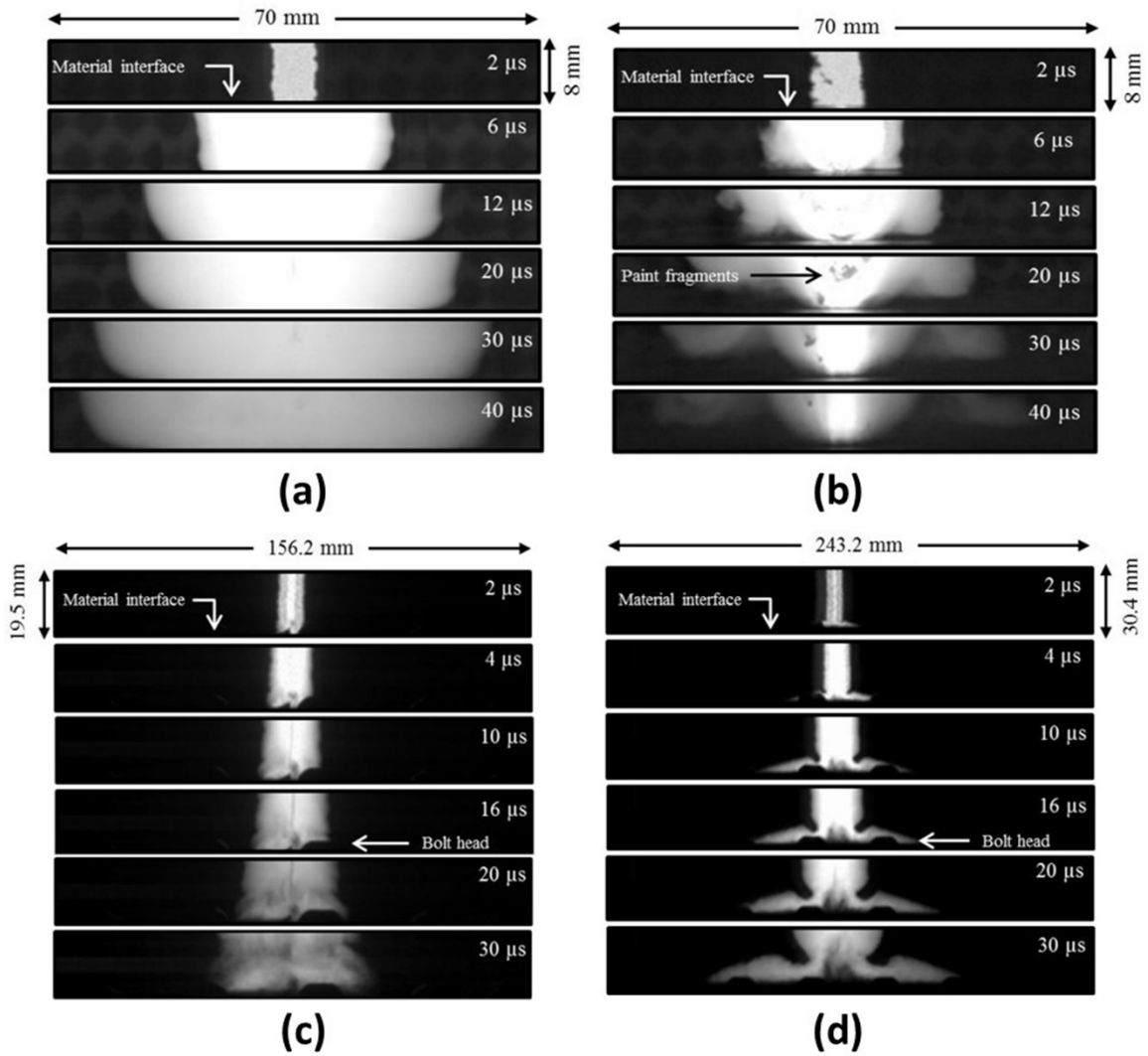


Fig. 2. Typical lightning-induced damage at a PRSEUS panel mid-bay location subjected to 124 kA peak current level. Adapted from [24]

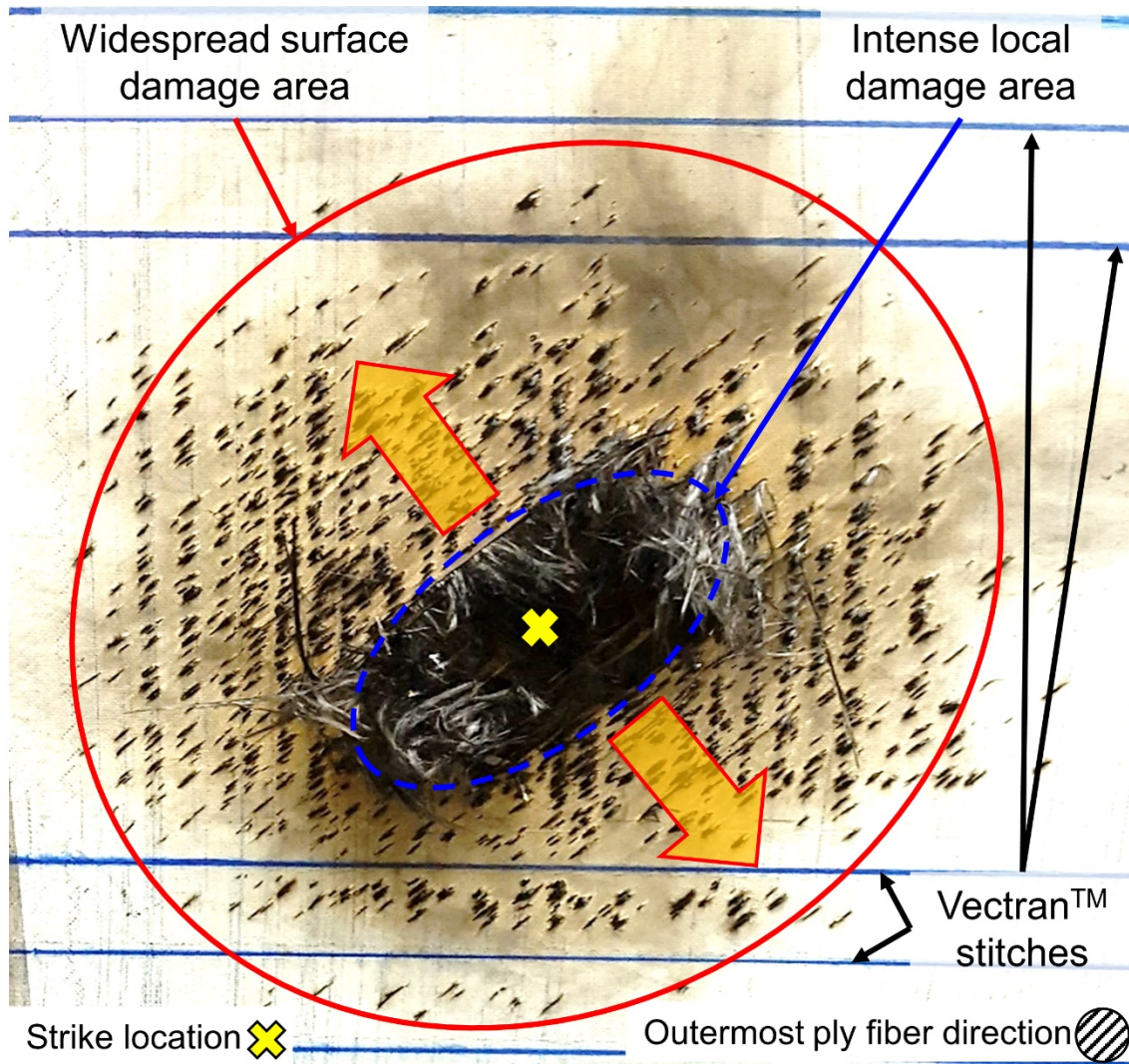


Fig. 3. Exploded view of a PRSEUS IML side preform assembly. Adapted from [32]

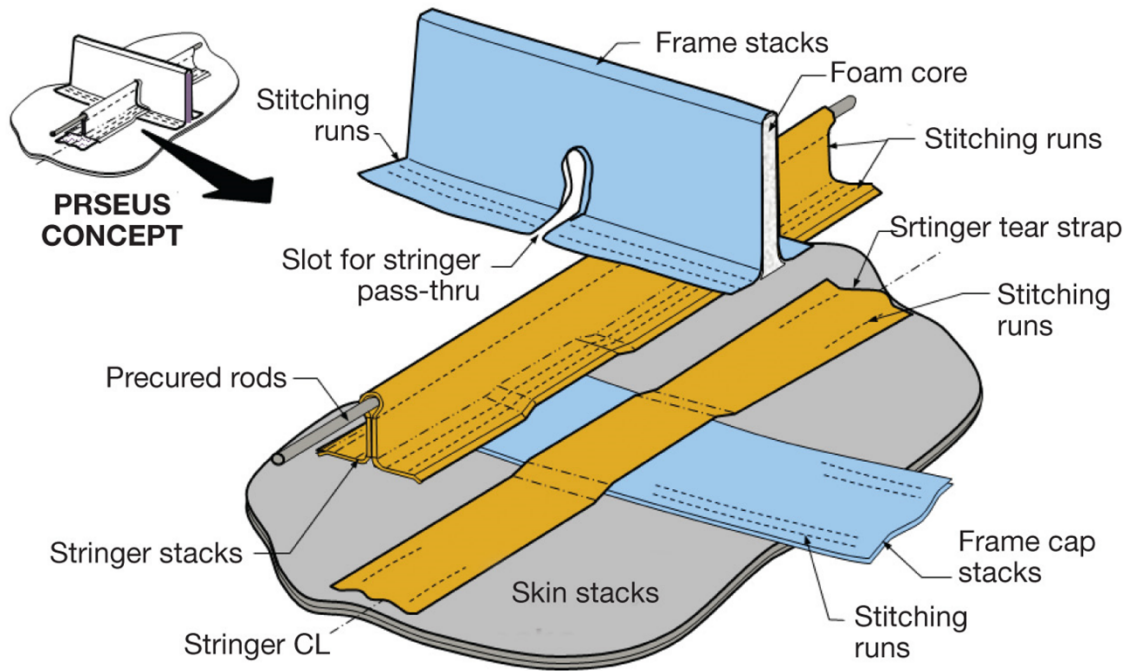


Fig. 4. (a) Impulse current generator setup, (b) top isometric view of the electrical components, (c) trigatron, and (d) electrical grounding condition of the PRSEUS panel.

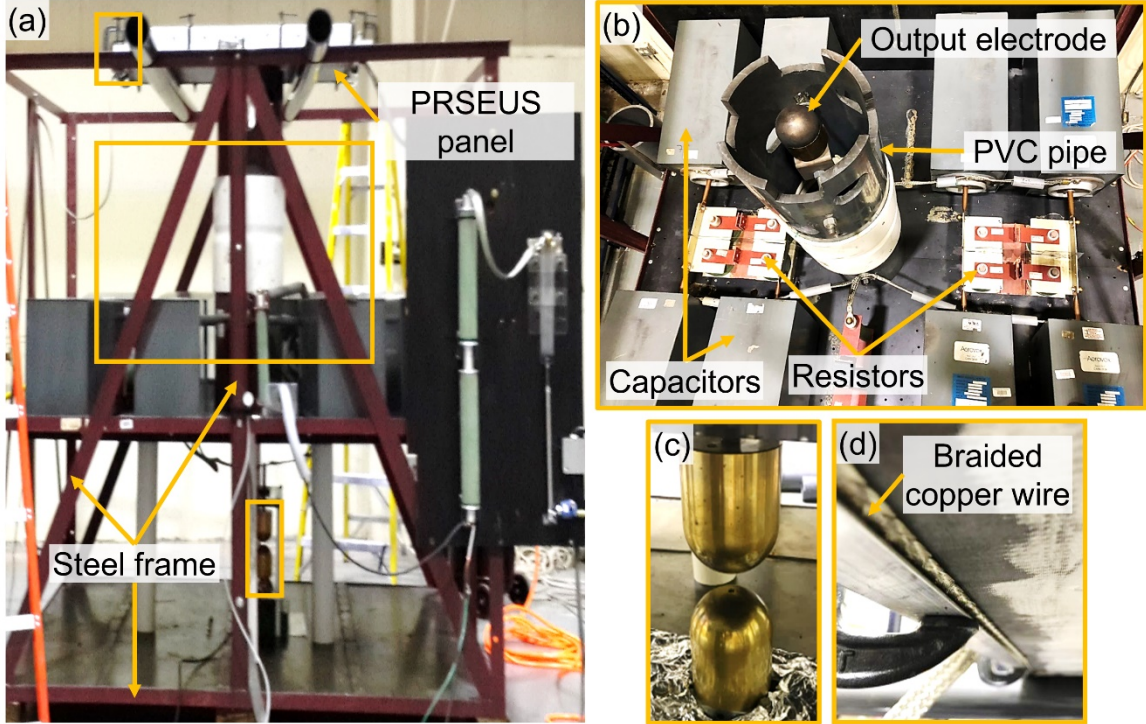


Fig. 5. (a) IML, and (b) OML side views of a pristine PRSEUS panel with a schematic of the intended lightning strike locations near the insulating boundaries.

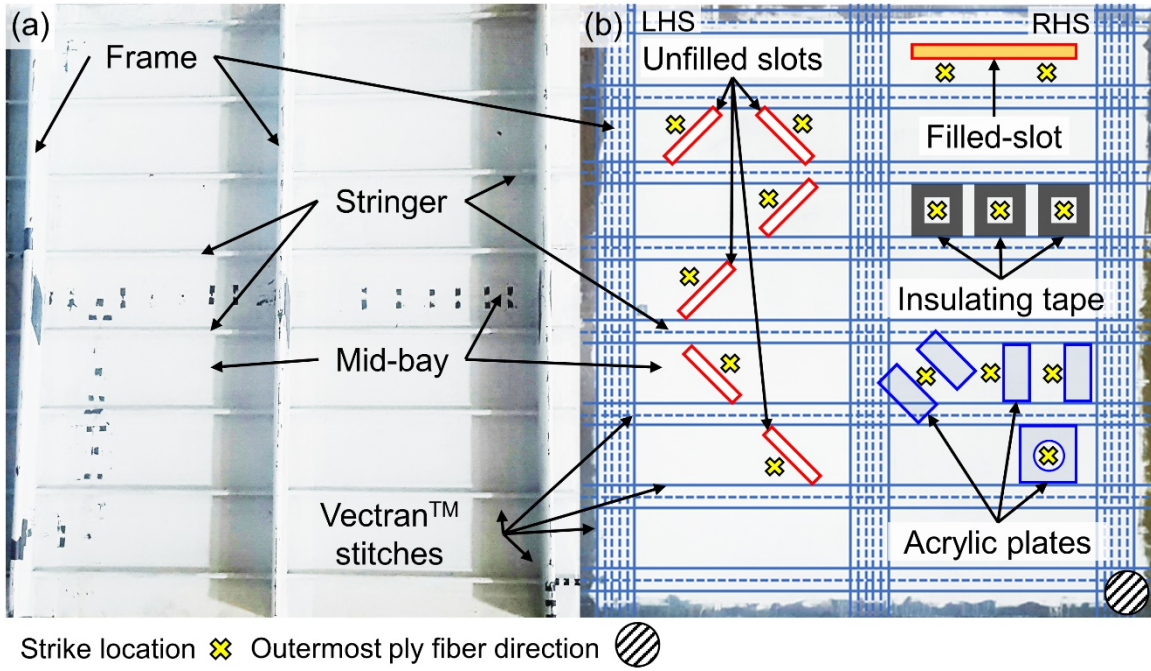


Fig. 6. Lightning strike damage adjacent to unfilled through slots oriented parallel to the outermost ply fiber direction due to peak currents of (a) 120 kA typical strike test setup, (b) 120 kA, (c) 118.4 kA, and (d) 136 kA.

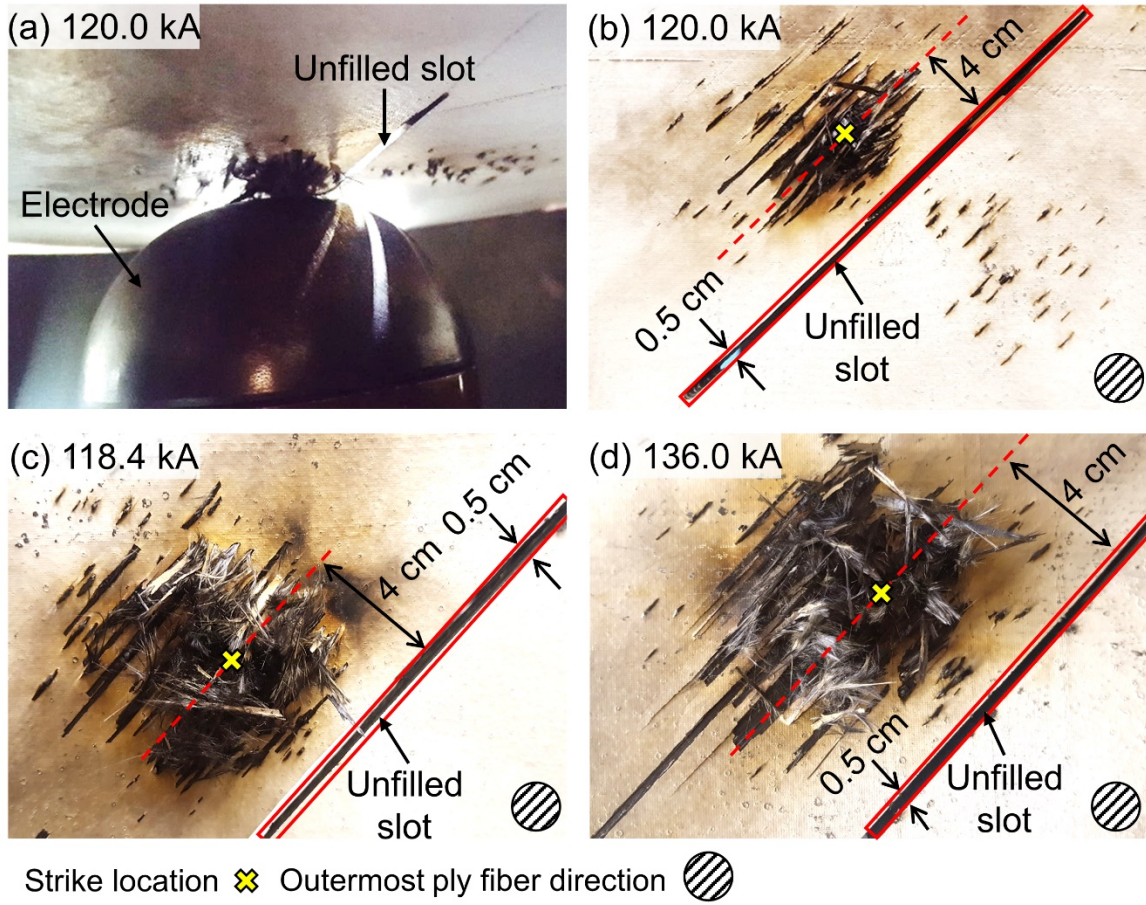


Fig. 7. Lightning strike damage adjacent to unfilled through slots oriented perpendicular to the outermost ply fiber direction due to peak currents of (a) 53.0 kA, (b) 117.0 kA, and (c) 120.0 kA.

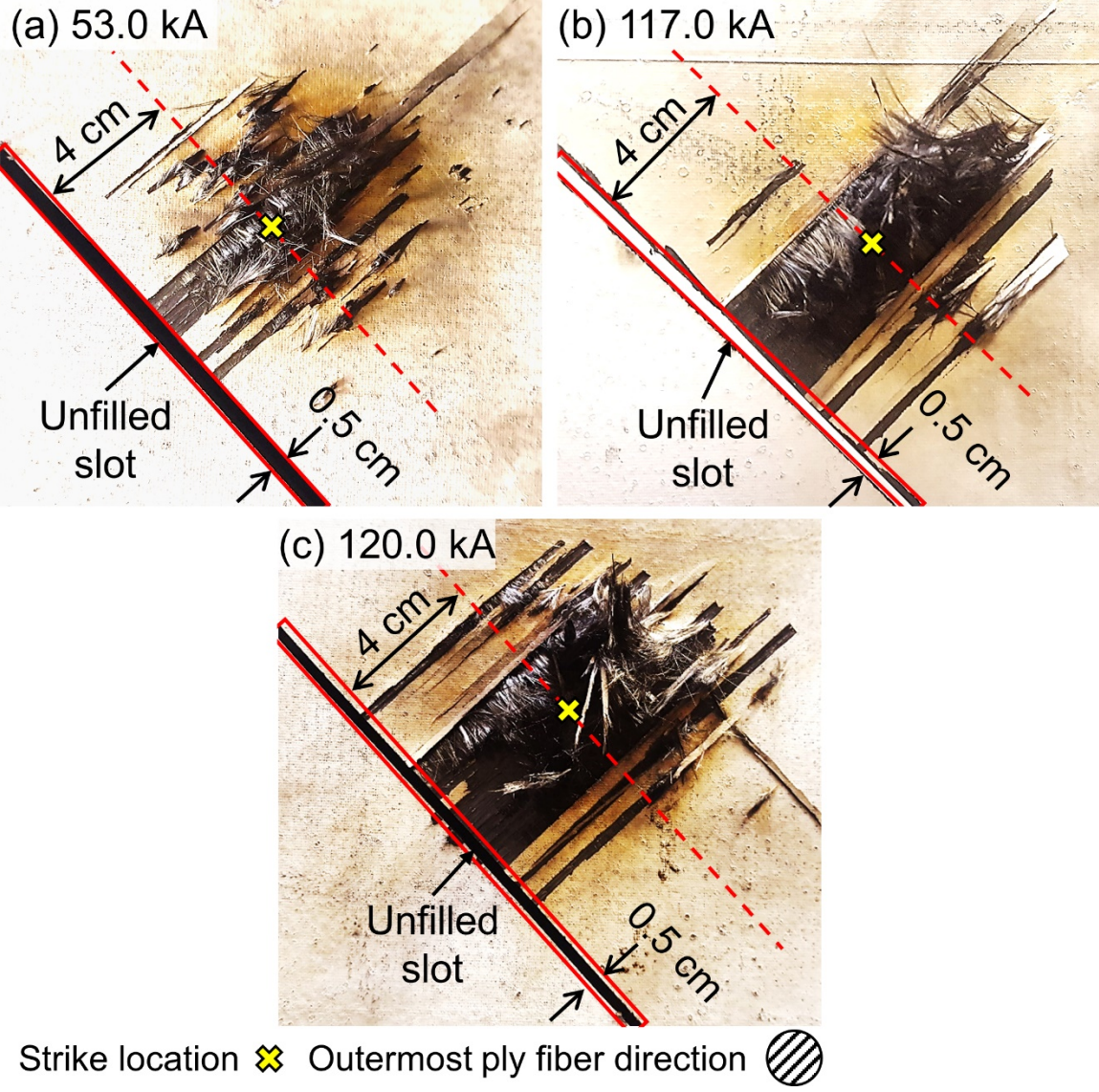


Fig. 8. Lightning strike damage adjacent to a horizontal slot parallel to the 0° fibers filled with non-conductive silicon paste due to peak currents of (a) 58.0 kA, and (b) 100.4 kA.

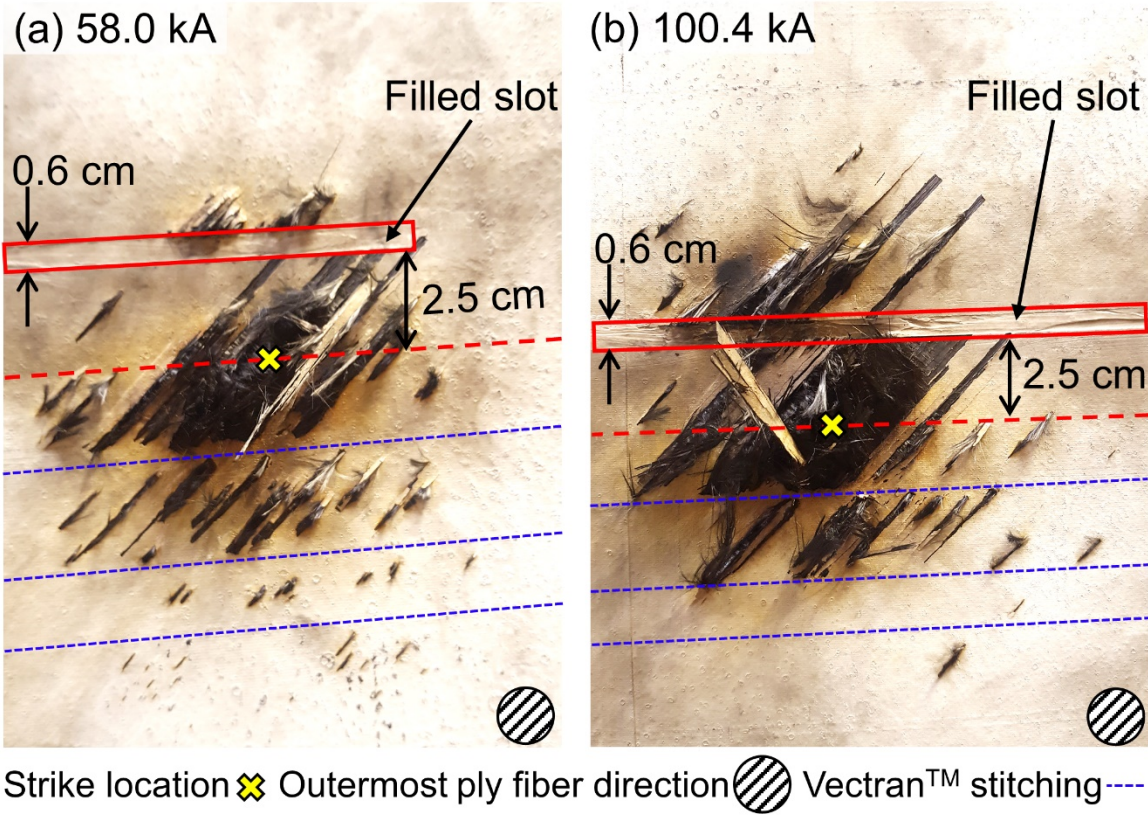


Fig. 9. Lightning strike damage at three mid-bay locations bounded by a non-conductive tape due to peak current levels of (a) 116 kA, (b) 116 kA, and (c) 126.0 kA.

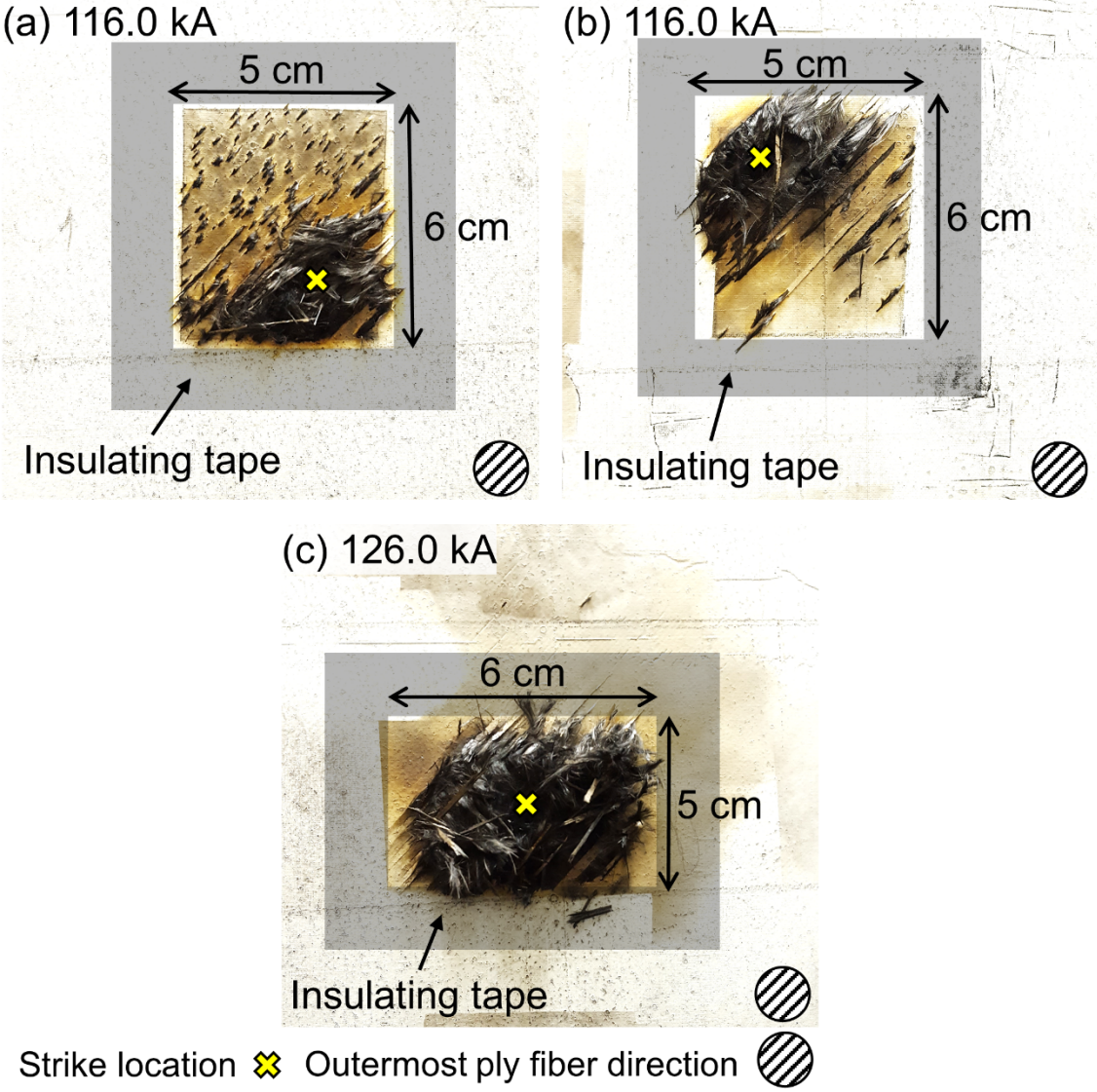
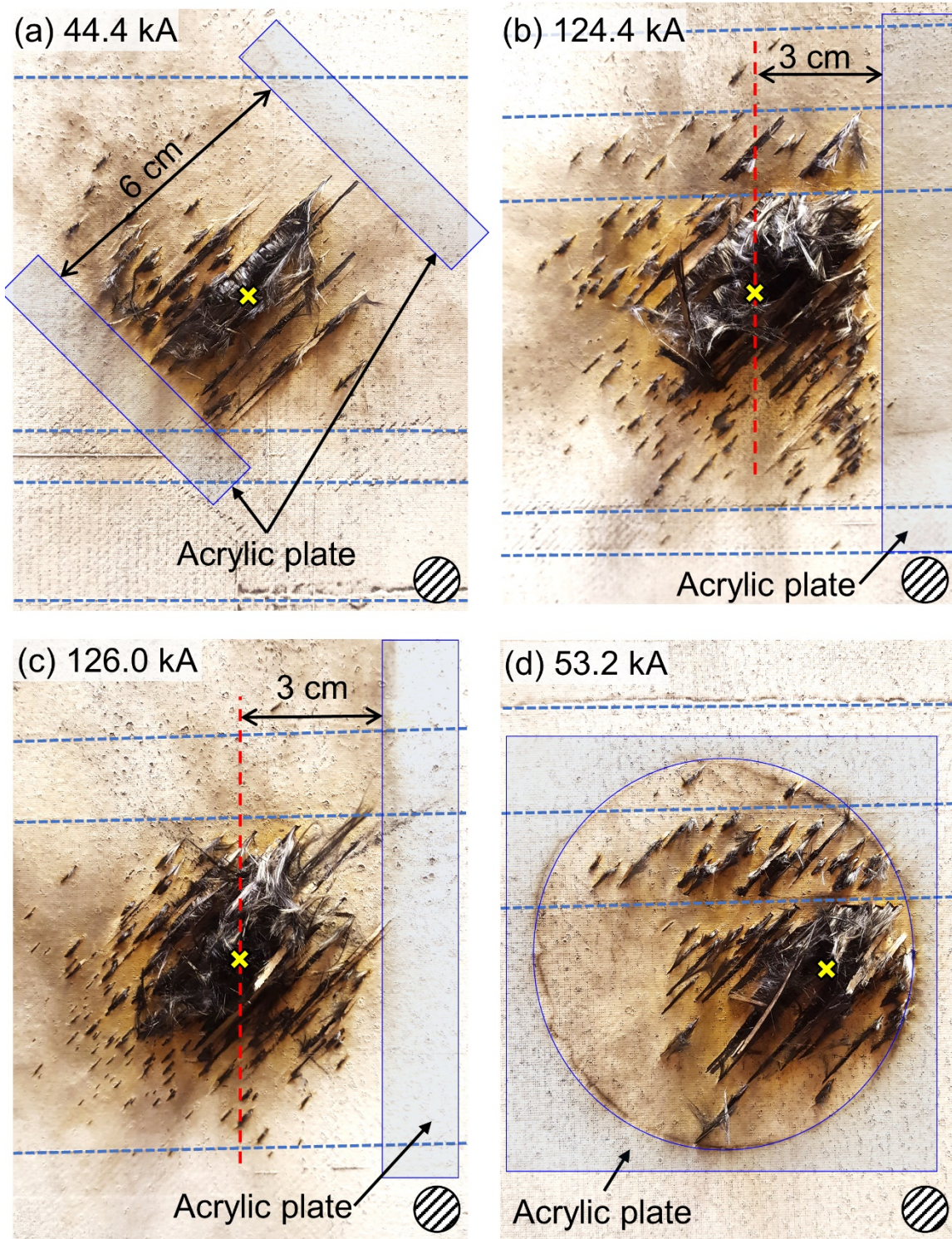




Fig. 10. Lightning strike damage to four mid-bay locations bounded by insulating acrylic plates positioned in different orientations with respect to the outermost ply fiber direction due to peak current levels of (a) 44.4 kA, (b) 124.4 kA, (c) 126.0 kA, and (d) 53.2 kA.



Strike location  Outermost ply fiber direction  Vectran™ stitching 